CODEN BIOIFW ISSN 0919-2719

bio images

Volume 11 Number 3-4 December 2003
Bioimaging Society

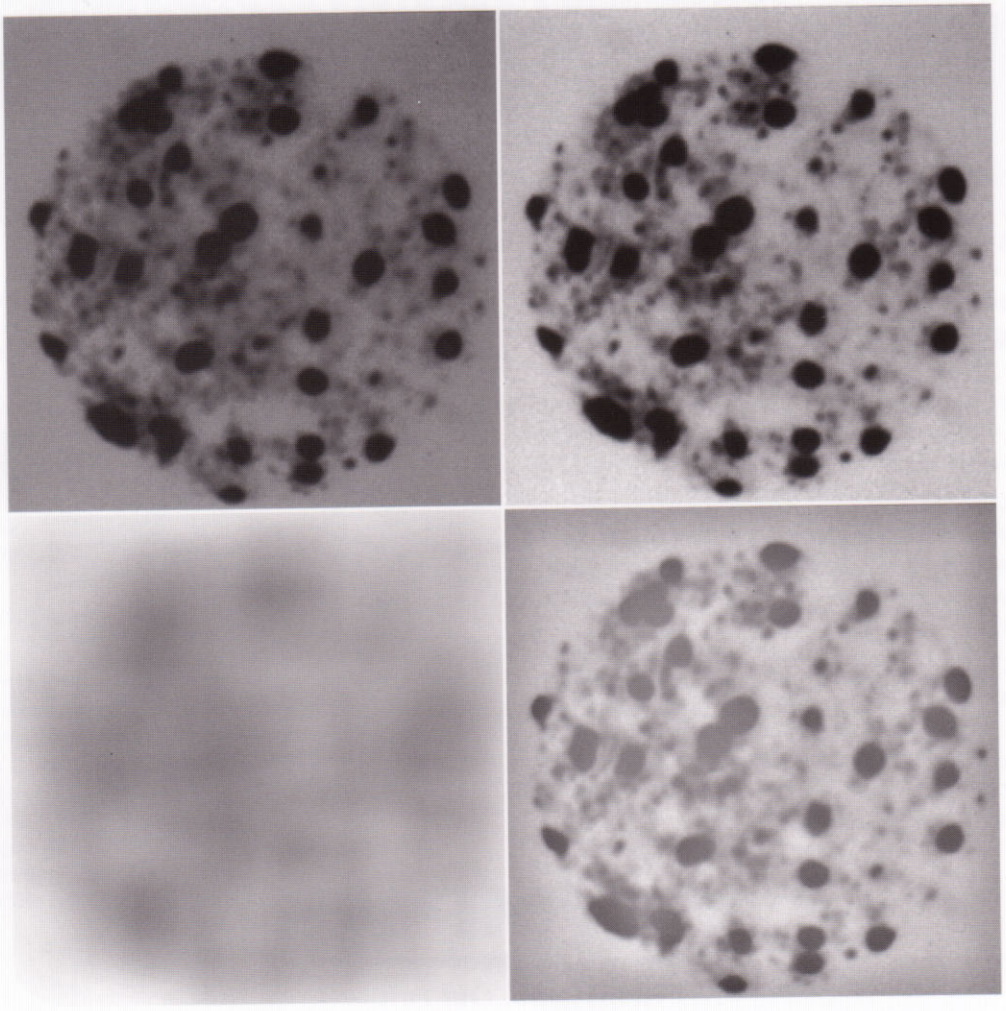

Bioimages 11 (3-4): 97–103, December 2003.

Quantitative Analysis of Nuclear Chromocenter in *Spiranthes sinensis* (Pers.) Ames.

Toshiyuki Wako[1] and Kiichi Fukui[2]*

[1]Department of Biochemistry, National Institute of Agrobiological Sciences, Tsukuba 305–8602, Japan, and
[2]Department of Biotechnology, Graduate School of Engineering, Osaka University, Suita, Osaka 565–0871, Japan.

Summary

The nucleus at interphase can be characterized by distinct morphological features and the distribution pattern of certain chromosomal regions such as nuclear chromocenters (CCs). Parameters of CCs within a nucleus are used to determine the type of resting chromosomes, which is a useful cytological characteristic that can serve as an indicator of cross-compatibility among orchid species. However, it is difficult using conventional imaging methods to identify the CCs within the interphase nucleus with the same level of acuity as human visual perception. This is because numerous variations on density and size are observed among CCs. An unsharp mask filter enables us to simulate human visual perception and allows us to identify CCs within the nucleus regardless of their density and size. As a result, CCs of *Spiranthes sinensis* (Pers.) Ames. were identified to the same standard as human visual recognition. Moreover, not only the quantitative parameters indicating morphological features but also the distribution pattern of CCs were successfully determined using this method. The numerical parameters of CCs can provide useful information not only for phylogenetic studies of Orchidaeceae but also for the future breeding of new hybrids of orchids.

Key words

Spiranthes sinensis, types of resting chromosomes, chromocenters (CCs), simulation of human vision, image analysis, distribution pattern

Introduction

It is well known that nuclei at interphase exhibit different distribution patterns of their heterochromatic chromocenters (CCs), which can be used as an indicator of the cytological characteristics of each strain, species, or genus, both in plants (Nagl, 1979) and in mammals (Haaf and Schmid, 1991). Tanaka (1971, 1977, 1987) categorized the distribution patterns of CCs within an interphase nucleus into seven types of "resting chromosomes". He showed that two species with similar types of resting chromosomes would occupy close phylogenic positions (Tanaka, 1971). Moreover, in orchids, species that share similar types of resting chromosomes show higher cross-compatibility than crosses between species with different types of resting chromosomes (Tanaka, 1971, 1987). Thus the use of this observation as an indicator to assess the cross-compatibility between two different species selected as parents for producing F1 hybrids shows great promise. In particular, it would be useful for orchid breeding, where new varieties are bred by cross-hybridization between phylogenetically distant species.

However, it is difficult to determine objectively the type of species among the seven types of resting chromosomes by visual inspection of the nuclei under a microscope alone. Therefore, individual biases in the visual determination of the types are unavoidable. Moreover, quantitative estimation and comparison of the types are almost impossible under ordinary visual inspection because comparison of data from different researchers is problematic. The most difficult part of objective typing is in the acquisition of reproducible and quantitative data on the chromocenters within the nucleus. The image data for the types of resting chromosomes can be separated into four parameters: the number of CCs; the area of CCs; the percentage of total area of CCs in a nucleus; and the distribution of CCs, which are represented by X and Y coordinates for the center of gravity (CG) of each CC.

In this paper, we describe application of an unsharp mask filtering (Ishida et al., 1982, 1983; Fukui et al., 1988), an imaging method that enables quantification of image parameters of CCs based on the mechanism of human visual perception, and also a method for analyzing the distribution pattern of CCs in interphase nuclei.

Materials and Methods

Nuclear image acquisition

A photographic image of a nucleus from root tissue of

*To whom all correspondence should be addressed.
E-mail: kfukui@bio.eng.osaka-u.ac.jp

Spiranthes sinensis (Pers.) Ames. (2n = 30) was a gift from Dr. Masashi Nakata (Botanical Gardens of Toyama, Japan). The original samples were prepared according to the method described by Tanaka (1969). Briefly, the root tips of *S. sinensis* were fixed in 45% acetic acid, macerated in a mixture of 45% acetic acid and 1N HCl (1:2), and stained with 2% aceto-orcein solution. The cytological samples were prepared by the squash method. Nuclear images without overlapped nuclear chromocenters (CCs) were photographed using black and white negative film (Neopan SS, Fuji) and then color positive film (Fujichrome, ISO100, Fuji).

Image analysis

The nucleus of *S. sinensis* image was digitized to produce an original digital gray image. This digitized image was then analyzed using a chromosome image analyzing system 3, CHIAS3 (Fukui, 1986; Kato and Fukui, 1998; Kato et al., 2003) as follows:

Step 1: The original gray image of the nucleus was produced by scanning the color positive film. The scanned image was reduced in size to a 256 × 256 pixel matrix and normalized to enhance the contrast.

Step 2: A reference image was produced by application of a low-pass filter (the matrix was 45 × 45 pixels in size with an equal value of 1 in every element) to the enhanced original image. The reference image was normalized and weighted by multiplication with a coefficient of 0.5. The weighted reference image was then subtracted from the enhanced original image. This filtering process is known as an unsharp mask method (Ishida et al., 1982, 1983). The setting of a proper gray value as the threshold for discrimination between the CCs and the background resulted in an appropriate discrimination of the CC regions. Subsequent binarization generated CC regions as a black area and the nuclear background as a white area (Fukui and Kamisugi, 1995). Minimal adjustments were interactively performed, such as separation of attached CCs. To demonstrate the effect of the unsharp mask method, image processing was also performed without this subtraction step.

Step 3: Four image parameters (the number of large and small CCs, the area of large and small CCs, the percentage of total area of CCs to a nucleus, and the X and Y coordinates for the centers of gravity (CGs) of CCs) were obtained by image analysis methods. Large and small types of CC were classified according to their areas. The area of the large CCs was larger than 100 pixels, whereas that of the small CCs was less than 50 pixels.

Step 4: To identify the pattern of CC distribution among random, aggregated, or regular distributions, the distance from a CG of a CC to the CG of its nearest CC was calculated on the nearest pair of the CGs of all the possible combinations of CCs, and the average distance between the pair from the nearest CG was obtained (Hopkins and Skellam, 1954). The original method developed by Hopkins and Skellam (1954) does not account for particle size, and thus is unable to deal with particles of different sizes. Thus, a computer simulation was developed in this study based on an Excel spreadsheet macro program. Ten thousand simulated nuclei were generated with the same number of large and small CCs randomly located within the nucleus. The sizes of simulated large and small CCs were approximated, and the averaged observed values were 187.8 pixels and 15.7 pixels, respectively. The mean distance between the CG of a CC and that of its nearest CC neighbor were also calculated for all CCs in the simulated nuclei. The mean values of the observed distance and simulated distances were then statistically tested to estimate the randomness of CC distribution.

Results and Discussion

Figure 1A shows an enhanced original image of the *S. sinensis* nucleus with a gray scale bar (gray value: 0, black and 255, white) at the top of the image. The image clearly shows that there are two types of CCs within the nucleus, large and small, which seem to be distributed almost evenly within the nucleus. No regions with a heavy concentration of large CCs or small CCs within the nucleus were observed, although some CCs were located very close to each other, as shown in Fig. 1A. This type of resting chromosomes is referred to as a "round prochromosome type" according to Tanaka (1987). However, it is difficult to count the exact number of both large and small CCs within the nucleus and to determine the randomness of CC distribution by visual inspection alone. Moreover, the application of the simple imaging method, which employs thresholding by a certain gray value, leads to erroneous results, as shown in Fig. 1B-D.

Figure 1B-D demonstrates the results of a simple discrimination of the CCs from the nuclear background by setting three thresholds of gray levels. When the gray value of 24 is set as the threshold to discriminate the CCs from the background nucleoplasm, 32 large CCs within the nucleus are extracted as the black regions after binarization (Fig. 1B). At the same time, most of the small CCs that were clearly observed by visual inspection in Fig. 1A are neglected, thereby identifying only 10 small CCs as shown in Fig. 1B. When a higher gray value setting of 54 is used as the threshold value, this results in an obvious increase in the number of small CCs, as shown in Fig. 1C. It is, however, still not possible to extract all of the small CCs that can be visually identified, especially those located in the peripheral regions of the nucleus. In contrast, CCs located in the darkly stained area of the

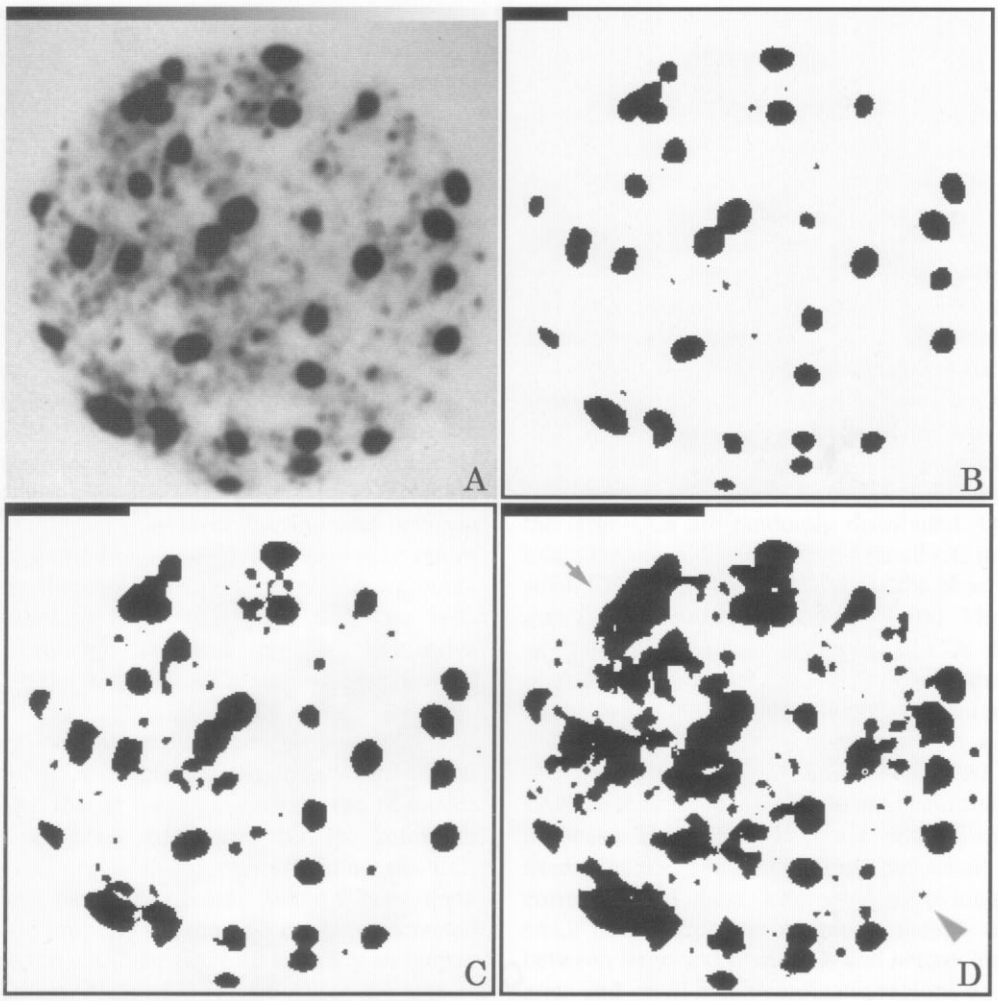

Fig. 1. Conventional thresholding for identifying the CCs. The normalized original image (A) was binarized by thresholding with a gray value of 24 (B), 54 (C) and 101 (D), respectively. An arrowhead indicates a small CC that was identified only by thresholding at a high gray value. An arrow indicates fused CCs.

nucleus begin to expand into the surrounding areas and to fuse with each other. This tendency is increased when a higher gray level of 101 is employed as the threshold value in order to identify the small CCs. For example, in Fig. 1D, the CC located at the right-hand periphery of the nucleus indicated by an arrowhead. This CC had higher gray values, and it could not be discriminated by high threshold values alone. Under these conditions, most CCs in the left-hand regions of the nucleus were fused to each other, forming large islands of heterochromatic regions, as indicated by an arrow. This is because the gray values of the background area near the cluster of large CCs (Fig. 1D, arrow) were lower than those of most of the small CCs.

This preliminary analysis indicates that it is difficult to extract large and small CCs evenly by the simple application of the imaging method setting the threshold at the certain gray value, although these small CCs are clearly observed by visual inspection even at the nuclear peripheral region. This fact clearly indicates that human visual perception employs a versatile thresholding system that allows the observer to discriminate between CCs and the nuclear background. It does not rely on a fixed threshold applicable to the whole nuclear region but uses local thresholds with different gray values varying from region to region in the nucleus. The thresholds for discrimination of dark and large CCs have a low gray level, and the thresholds for light and small CCs have a high gray level. Fukui and Kamisugi (1995) reported a similar phenomenon in the visual recognition of differently sized chromosomal bands after C-band treatment of *Crepis* chromosomes. Kato et al. (2003) also employed a similar versatile method to identify the condensed regions within chromomeres in a rice pachytene chromosome. In fact the method is known as the unsharp mask method, which has been used for enhancement of contour lines in radiographic images (Ishida et al., 1982, 1983). A flexible and region-specific setting of gray level must be a characteristic of human vision that allows for the

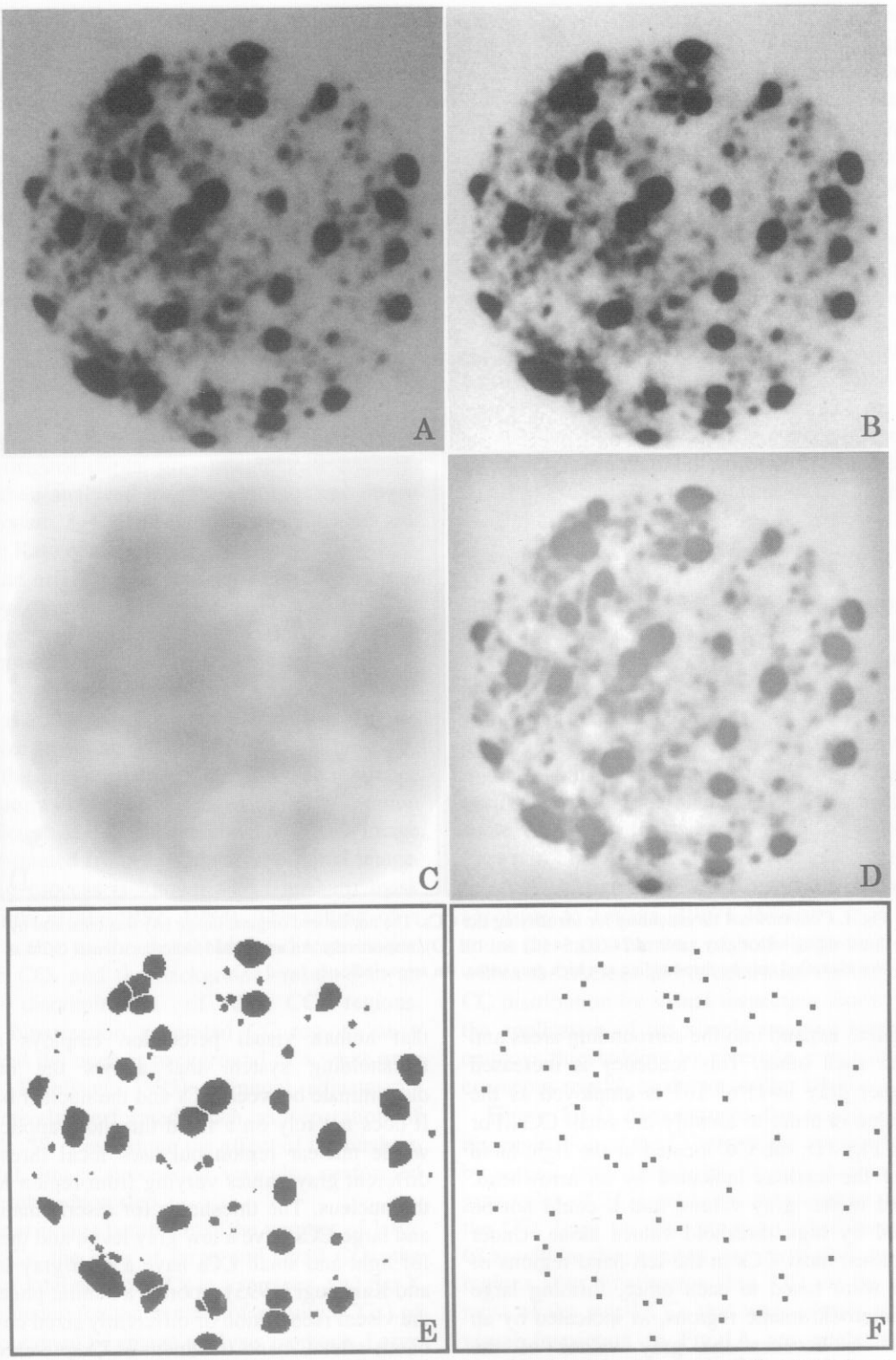

Fig. 2. A method for identifying the CCs by emulating the human visual perception mechanism. (A) Original digitized image. (B) Enhanced original image. (C) Low-pass filtered image. (D) Subtraction. (E) Thresholding and binalization were applied. (F) Gravity of each CC.

proper recognition of all the CCs regardless of their size and gray level (Fukui and Kamisugi, 1995).

The unsharp mask method is a simple but adequate imaging method that allows simultaneous recognition of large and small CCs within the nucleus by mimicking the system of human visual perception (Fig. 2). Gray values of the background were normalized to localize thresholds varying from region to region in the whole

area of the image. This approach is different from other imaging methods to enhance S/N ratio or to enhance edge contrast. An enhanced original image with a higher contrast (Fig. 2B) was produced by normalization of the original nuclear image (Fig. 2A). Then a low-pass filter was applied to the enhanced original image to produce the reference image (Fig. 2C), which was then used for the adjustment of local density distribution according to the distribution of gray values within the nucleus. The image was normalized and the gray value of each pixel was multiplied by 0.5 to weight the gray value of each pixel. This weighted reference image was used as the standard in the discrimination of the CCs from the nuclear background. The subtraction of the weighted reference image from the enhanced original image generates Fig. 2D. The setting of a threshold value with the proper gray level discriminates between CCs and background regions. Regions with gray values less than the threshold are regarded as background. After binarization, large and small CCs are both adequately extracted as black regions. Interactive separation of the attached CCs was also performed (Fig. 2E).

The critical parameters for appropriate extraction of both types of CCs evenly are the matrix size of the low-pass filter that is used to generate the reference image, the weighting coefficient for the reference image, and the gray value for thresholding the CCs regions from the background. When these three parameters are properly set, the CCs could be extracted and perceived to a similar level of accuracy as human visual perception. A suitable matrix size is the root of the attached and largest CC area in pixels. In other words, differences between individual observers or bias caused by differences in visual perception may be quantified by these three parameters.

The CCs are distinguished and grouped into 32 large and 37 small CCs based on their area. The large and small CCs are 187.8 and 15.7 pixels in area on average, respectively. The area of total, large, and small CCs occupies 14.3, 13.0, and 1.3% of the total nuclear area, respectively. Positions of the CG of each CC were also calculated, and CG positions are marked in the nucleus (Fig. 2F).

Usefulness of the unsharp mask method was demonstrated using fluorescent image of barley interphase nuclei (Fig. 3). Nucleoli could not be discriminated from the original gray image (Fig. 3A) by simple application of single threshold, because the nucleolar regions had higher brightness than nuclear edge. Thus the application of the gray level that is suitable for discrimination of the nuclear area results in the loss of nucleolar identification (Fig. 3B). The unsharp mask method was applied to this image with 91×91 pixels of matrix based on the approximate nucleolar size (91 pixel in diameter) (Fig. 3C). Adequate threshold enables us to remove background and nucleolar regions (Fig. 3D).

The distribution pattern of the CCs was then quantified based on the mean distances from a CG to the CG of the nearest CC (Table 1). From ten thousand simulated nuclei, the upper and the lower confidence limits (95%) were calculated. If the nearest distance of the observed nucleus is higher or lower than the upper or the lower limits, then randomness of distribution can be rejected. The mean distance from a CG to the CG of the nearest CC among all the possible combinations of CCs in both the observed and simulated nuclei does not show a significant difference, indicating that all the CCs are randomly scattered in the nucleus in the case of *S. sinensis*. Statistical analysis of mean distance from a large CC to the nearest large CC indicates that the large CCs are randomly distributed. On the other hand, the mean distance from a small CC to the nearest small CC is significantly shorter in the observed nucleus than in the simulated nuclei ($P < 0.05$). Therefore, this analysis indicates that only the small CCs show a weak tendency to be closely located to each other, although on the whole the CCs are randomly scattered.

S. sinensis has 20 chromosomes with a heterochromatic long arm and 30 chromosomes with about 80 small heterochromatic regions on euchromatic arms in prophase. This number depends on the *S. sinensis* lines used (Tanaka, 1969). The large and small CCs would correspond to these heterochromatic long arms and small heterochromatic regions, although the numbers between large and small CCs and heterochromatic long arms and small heterochromatic regions do not exactly agree. Some heterochromatic long arms may divide into two or more large CCs at interphase. Less than half of the small heterochromatic regions observed on euchromatic arms can be attributed to constitutive heterochromatin because about 40 small CCs were observed at interphase. Barley and rye showed typical clusters of CCs within interphase nuclei that reflect the Rabl orientation of chromosomes (Anamthawat-Jónsson and Heslop-Harrison, 1990; Wako et al., 2002). However, a random distribution of large CCs was observed in *S. sinensis*, indicating a random distribution of the chromosomes within the nucleus. Weak aggregation of small CCs would indicate synteny of small heterochromatic regions within the same arms of the chromosomes.

As a result, it is concluded that the CCs of *S. sinensis* are random in their distribution. Here both the unsharp mask method for identification of CCs and the method currently developed for the analysis of their distribution pattern in the nucleus were effective. In addition, application of the unsharp mask method is effective to discriminate the nucleolar region from the nuclear background, as shown in the fluorostained barley nucleus. It is anticipated that this imaging

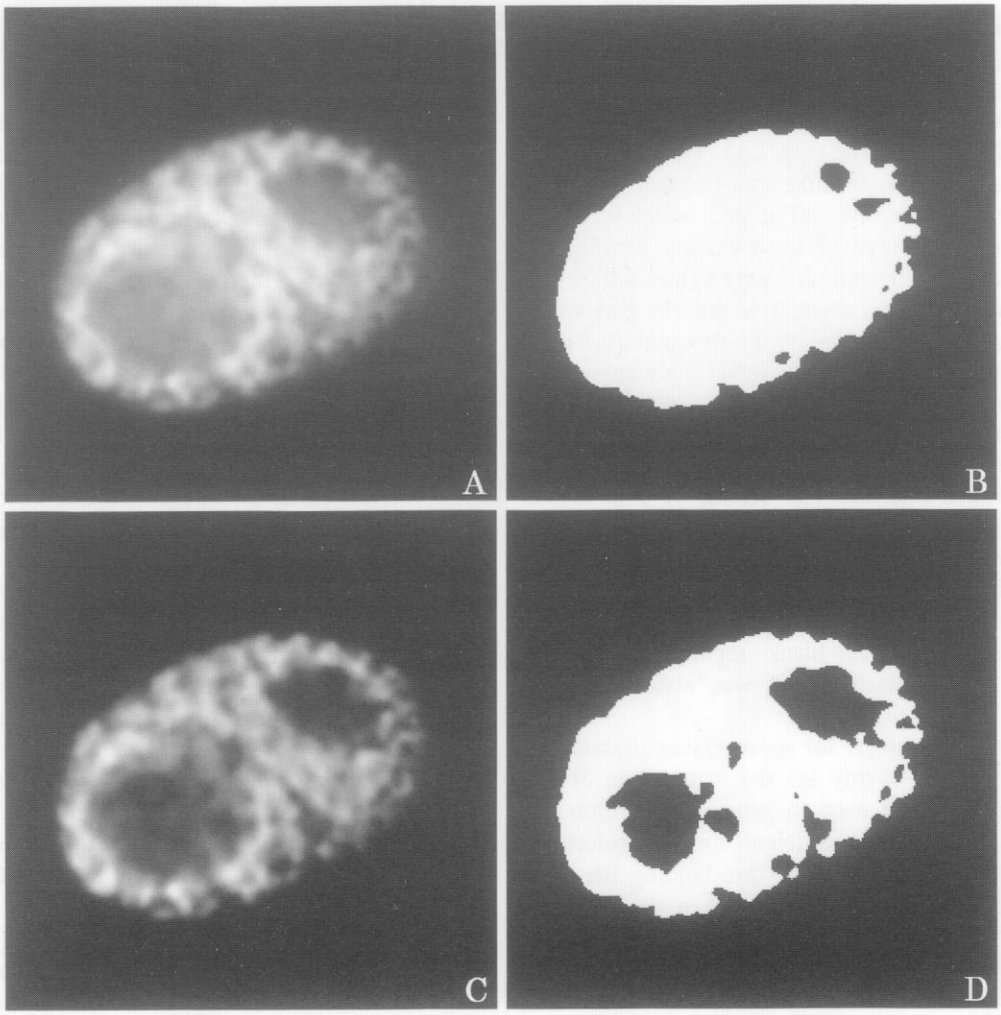

Fig. 3. Effectiveness of the unsharp mask method for identification of nucleolar and nuclear regions. (A) Original fluorescent image of barley nucleus. (B) Binarized image of A after thresholding. (C) The image after unsharp mask filtering. (D) Binarized image of C after thresholding.

Table 1. The nearest distances for the observed nucleus and the ten thousand simulated nuclei.

	Observed nucleus	Simulated nuclei	Lower limit	Upper limit
All CC	15.66	15.88	14.57	17.18
Large CC	25.00	24.12	21.64	26.75
Small CC	15.62*	19.00	15.73	22.33

*Significant (P = 0.05).

method could provide reproducible and objective parameters to assist in the evaluation of cross-compatibility between two arbitrary species to be hybridized.

Acknowledgments

This study was supported by Grants-in-Aid from the Special Coordination Fund of the Ministry of Education, Culture, Sports, Science and Technology, Japan, to K.F.

Received November 21 2003; revised January 15 2004.

References

Anamthawat-Jónsson, K. and Heslop-Harrison, J.S. (1990). Centromeres, telomeres and chromatin in the interphase nucleus of cereals. Caryologia, 43: 205–213.

Fukui, K. (1986). Standardization of karyotyping plant chromosomes by a newly developed chromosome image analyzing system (CHIAS). Theor. Appl.

Genet., 72: 27–32.

Fukui, K. and Kamisugi, Y. (1995). Mapping of C-banded *Crepis* chromosomes by imaging methods. Chromosome Res., 3: 79–86.

Fukui, K., Tsujimoto, H. and Noda, K. (1988). Imaging techniques for wheat karyotyping. Proc. 7th. Intl. Wheat Genet. Symp. 1: 275-280.

Haaf, T. and Schmid, M. (1991). Chromosome topology in mammalian interphase nuclei. Exp. Cell. Res., 192: 325–332.

Hopkins, B. and Skellam, J.G. (1954). A new method for determining the type of distribution of plant individuals. Ann. Bot., 18: 213–227.

Ishida, M., Frank, P.H., Doi, K. and Lehr, J.L. (1983). High quality digital radiographic images: Improved detection of low-contrast objects and preliminary clinical studies. RadioGraphics, 3: 325–338.

Ishida, M., Kato, H., Doi, K. and Frank, P.H. (1982). Development of a new digital radiographic image processing system. Proc. Soc. Photo-Opt. Instrum Eng., 347: 42–48.

Kato, S. and Fukui, K. (1998). Condensation pattern (CP) analysis of plant chromosomes by an improved chromosome image analyzing system, CHIAS III. Chromosome Res., 6: 473–479.

Kato, S., Ohmido, N. and Fukui, K. (2003). Development of a quantitative pachytene chromosome map in *Oryza sativa* by imaging methods. Genes Genet. Syst., 78: 155–161.

Nagl, W. (1979). Nuclear ultrastructure; condensed chromatin in plants is species-specific (karyotypical) but not tissue-specific (functional). Protoplasma, 100: 53–71.

Tanaka, R. (1969). Deheterochromatinization of the chromosomes in *Spiranthes sinensis*. Jpn. J. Genet., 44: 291–296.

Tanaka, R. (1971). Types of resting nuclei in Orchidaceae. Bot. Mag., 84: 118–122.

Tanaka, R. (1977). Recent karyotype studies. In: Plant Cytology (Ogawa, K. eds.), Asakura Book Co. Ltd., pp. 293–326.

Tanaka, R. (1987). The karyotype theory and wide crossing as an example in Orchidaceae. In: Plant Chromosome Research 1987, Proc. Sino-Japan Symp. Plant Chromosomes (Chen, R.Y. and Tanaka, R. eds.), Universal Academy Press, pp.1–10.

Wako, T., Furushima-Shimogawara, R., Fukuda, M., Belyaev, N.D. and Fukui, K. (2002). Cell cycle dependent and lysine residue-specific dynamic changes of histone H4 acetylation in barley. Plant Mol. Biol., 46: 645–653.